American Mineralogist, Volume 63, pages 1175–1181, 1978

Surite, a new Pb-rich layer silicate mineral

KITARO HAYASE[1], JORGE A. DRISTAS

Departamento de Geologia, Universidad Nacional del Sur
Bahia Blanca, Argentina

SADAO TSUTSUMI

Institute of Earth Science, School of Education
Waseda University, Tokyo 160, Japan

RYOHEI OTSUKA, SACHIO TANABE

Department of Mineral Industry, School of Science and Engineering
Waseda University, Tokyo 160, Japan

TOSHIO SUDO

3-20-7 Miyasaka, Setagaya-ku, Tokyo 156, Japan

AND TSUTOMU NISHIYAMA

Natural Science Laboratory, Toyo University, Tokyo 112, Japan

Abstract

Surite, $Pb(Pb,Ca)_{1.17}(CO_3)_2(Al,Fe,Mg)_2(Si_{3.67}Al_{0.33})O_{10}(OH)_2$ is a new clay-mineral species occurring as compact aggregates in the oxidation zone of the lead–zinc–copper deposits of the Cruz del Sur mine, Argentina. Surite is monoclinic, $a = 5.22$, $b = 8.97$, $c = 16.3$A, $\beta = 96.1°$, $Z = 2$; the space group is possibly $P2_1$. Color white, luster glossy like talc; streak white, cleavage perfect {001}. Hardness (Mohs) 2–3, density (g/cm³) 4.0 (meas). Optically anisotropic, colorless in thin section; refractive indices $\alpha = 1.693(2)$, $\gamma = 1.738(2)$; parallel extinction and positive elongation. The wet-chemical analysis gave SiO_2 23.58, Al_2O_3 11.27, Fe_2O_3 0.41, CaO 4.75, MgO 1.29, K_2O none, Na_2O 0.77, H_2O+ 3.33, H_2O- 0.39, PbO 45.32, CuO 0.07, CO_2 9.45, sum 100.63 percent. The X-ray powder pattern is characterized by a 16A reflection and its integral series to the 11th order. These reflections do not expand upon ethylene glycol treatment. The X-ray powder study and chemical analysis of the dried acid-treated residue showed that this residue corresponds to a dioctahedral smectite. DTA-TG curves in air show an endotherm around 600° accompanied by weight loss, two exotherms at about 700° and 800°, and an endotherm in the 700–800°C region. The two exotherms are not recognized in nitrogen. IR-spectra are composed of the absorption bands of a silicate and carbonate. The structure of surite is based upon a cerussite-like layer with vacant sites for Pb intercalating with a 2:1 silicate layer similar to dioctahedral smectite. The name is for the locality.

Introduction

The new mineral has been found in the oxidation zone of the lead–zinc–copper deposits of the Cruz del Sur mine, Argentina. Mineralogical investigation indicated that the mineral is a new Pb-rich layer silicate. The name of the mineral derives from the mine. The species and name have been approved by the Commission on New Minerals and Mineral Names, IMA.

The type specimen is preserved at Institute of Earth Science, School of Education, Waseda University.

[1] Died on March 17, 1977.

0003-004X/78/1112-1175$02.00

Table 1. Chemical compositions of surite and its residue after treatment with hydrochloric acid

	(1)		(2)*
SiO_2	23.58	SiO_2	55.38
Al_2O_3	11.27	Al_2O_3	27.46
Fe_2O_3	0.41	Fe_2O_3	1.61
CaO	4.75	CaO	0.95
MgO	1.29	MgO	3.68
Na_2O	0.77	Na_2O	0.09
K_2O	---	K_2O	tr.
$H_2O(+)$	3.33	$H_2O(+)$	10.11
$H_2O(-)$	0.39		
PbO	45.32		
CuO	0.07		
CO_2	9.45		
Total	100.63	Total	99.28

(1) Untreated
(2) The residue obtained from the sample powder pre-treated with 0.75 % hydrochloric acid, dried at 110°C.
* *The residue was contaminated with a small amount of Fe_2O_3.*

Mode of occurrence

The Cruz del Sur mine is situated at about 42 km ESE of Los Menucos, Rio Negro province, Argentina (40°50′S, 68°07′W). The lead–zinc–copper deposits occur as fissure-filling veins, 1–5 m wide, N35°E in strike and almost vertical in dip, at the boundary between andesite and rhyolite. The veins have been exploited only about 60 m along the strike and about 15 m along the dip in the oxidation zone. The oxidation zone contains many secondary minerals such as cerussite, anglesite, malachite, azurite, atacamite, paratacamite, mottramite (Hayase and Dristas, 1972), wulfenite, vanadinite, chalcocite, digenite, limonite, opal, galena, hematite, calcite, and gypsum. Almost all parts of the oxidation zone are stained reddish-brown with iron oxide and hydroxide minerals. Wall rocks have suffered sericitization, chloritization, and carbonatization. Surite is found as compact aggregates occurring in veinlets, 50 mm in maximum thickness, in the oxidation zone.

Macroscopic properties

The compact aggregates are heavy, white to pale green, and are glossy like talc. Hardness is 2–3. The powdered mineral effervesces in 0.75 percent HCl at room temperature; HCl treatment at room temperature for 7 days produces a gel-like residue about 40 percent by weight of the original material. Microchemical tests showed a large amount of lead in the filtrate. The measured density is 4.0 g/cm^3, much higher than that of common silicate minerals and lower than that of cerussite.

Preliminary X-ray diffraction analysis revealed a strong 16A reflection and its higher orders. In the patterns of some samples, weak reflections due to impurities such as kaolinite, cerussite, and quartz are discernible.

Optical properties

Thin-section study revealed that the mineral consists of aggregates of tabular lath-shaped crystals with good cleavage parallel to the elongation, which shows positive sign. The refractive indices measured by the oil-immersion method are as follows: α = 1.693, γ = 1.738 ($\pm$0.002); $\gamma-\alpha$ = 0.045–0.047. These values are much lower than those of cerussite and higher than those of common clay minerals.

Chemical composition

The chemical composition is given in Table 1. The CO_2 analysis was performed as follows: HCl was added to the sample powder and the CO_2 produced was passed into 10 percent $BaCl_2$ solution (with ammonia). The $BaCO_3$ precipitate was filtered, dried and weighed. From the weight, the content of CO_2 was calculated. The residue after treatment with HCl was dried at 110°C and analysed (Table 1). This treatment completely removes PbO and CO_2, and the composition of the residue is close to that of a montmorillonite mineral. The chemical composition shows that the mineral can be regarded as a 2:1 dioctahedral smectite interlayered with lead carbonate.

Electron-optical investigation

Scanning electron micrographs show aggregates of flaky crystals (Fig. 1). The electron diffraction pattern of a crystal with its (001) plane on the substrate consists of distinct spots in hexagonal symmetry [Fig. 2(A)]. Electron diffraction of polycrystalline aggregates gave several powder rings, as shown in Figure

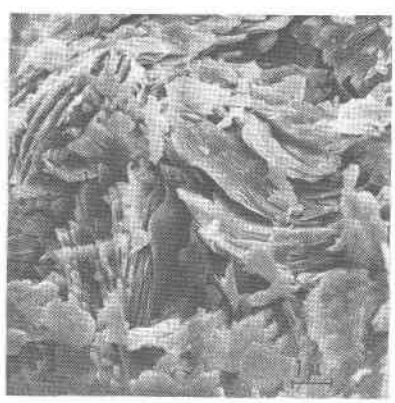

Fig. 1. Scanning electron micrograph of surite.

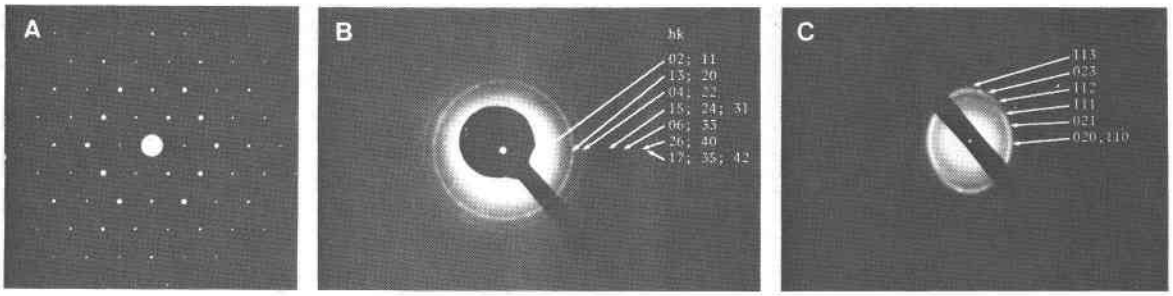

Fig. 2. Electron diffraction patterns from oriented crystal deposits on a colloidal membrane. (A) A crystal (normal to the specimen substrate); (B) polycrystalline aggregates (normal to the substrate); (C) oblique texture pattern obtained from the specimen substrate tilted 40° from normal.

2(B). The *hk* indices and spacings, calibrated with the patterns of gold, are given in Table 2(I). The specimen substrate was tilted to give an oblique-texture pattern [Fig. 2(C)]. The monoclinic lattice parameters, $a = 5.22$, $b = 8.97$, $c = 16.3$A, $\beta = 96.1°$, could be determined on the basis of the spacings and indexing of these rings and arcs with aid of the X-ray powder-diffraction pattern. The parameters are calculated from the following three factors: (a) $c\sin\beta =$ 16.2A, obtained from the X-ray powder pattern; (b) $a\sin\beta = 5.19$, $b = 8.97$A, obtained from the electron diffraction rings [Table 2(I)]; and (c) $d(111) = 4.32$A, obtained from an arc in the oblique-texture pattern [Table 2(II)].

X-ray powder-diffraction pattern

Most reflections in the diffraction pattern (Table 3 and Fig. 3) can be indexed as an integral series of basal reflections corresponding to a spacing of 16.2A up to the 11th order (1.470A), and some peaks can be indexed as prism reflections of a phyllosilicate with d = 4.48 (110,020), 2.590 (200,130), 2.247 (203,220), 1.697 (310,240,150), and 1.497 (330,060). Some extremely weak and broad peaks are also discernible.

Table 2. Indices and spacings obtained from electron diffraction patterns of oblique textures

(I)		(II)		
hk indices	d_{obs}(A)	*hkl*	d_{obs}(A)	d_{calc}(A)
02;11	4.49	020;110	4.49	4.49*
13;20	2.60	021	4.37	4.33*
04;22	2.24	111	4.23	4.23
15;24;31	1.70	112	3.73	3.79*
06;33	1.50	023	3.47	3.45*
26;40	1.30	113	3.31	3.31*
17;35;42	1.24			

* *obtained on the basis of the lattice parameters: a=5.22 A, b=8.97 A, c=16.3 A, β=96.1°, which are obtained from the following three factors: (a) csinβ=16.2 A as obtained from the X-ray powder pattern, (b) asinβ=5.19 A, b=8.97 A as obtained from this Table (I), and (c) d(111)=4.23 A selected from this Table (II)*

Treatment with ethylene glycol does not cause discernible changes in intensities and spacings of overall peaks. The pattern does not display the characteristic reflections of cerussite. With a two-dimensional orthogonal lattice, the unit-cell parameters are a = 5.17, $b = 8.97$, $d(001) = 16.2$A.

The microscopic and electron optical studies strongly suggest that the material is monomineralic and free from impurities. The residue was dried at room temperature and its X-ray diffraction pattern agrees with that of a smectite (Fig. 3). The 13.6A

Table 3. X-ray powder diffraction data for surite

d (A)*	*hkl***	I/I_0*	I/I_0***
16.2	001	68	100
5.4	003	71	26
4.48	110;020	20	21
4.35	021	12	10
4.05	004	100	30
3.705	014	5.5b	9
3.573	103	8b	
3.463	023	11b	12
3.240	005	60	17
3.035	104	7.5	5
2.700	006	35	6
2.590	200;130	18	18
2.313	007	50	9
2.247	203;220	14b	14
2.079	204	4.5b	13
2.056	027;$\bar{1}$41	4.5b	
2.024	008	7	1
1.984	117	3b	13
1.951	$\bar{1}$43	3b	
1.800	009	5	0.2
1.697	310;240;150	4b	5
1.618	00,10	4b	7
1.581	$\bar{1}$54;$\bar{2}$28	3b	
1.497	330;060	3.5b	2.5
1.470	00,11	4b	-

* *b: broad; Cukα, Ni-filtered, 35 kV, 12 mA, scanning speed 2 cm per minute, ratemeter ×16, multiplier ×1, time constant 2 sec, slit system 1°-1°-0.2 mm*

** *indices estimated on the basis of the lattice parameters, a=5.22 A, b=8.97 A, c=16.3 A, β=96.1° determined mostly employing electron diffraction data*

*** *relative intensities obtained by applying the slit-correction*

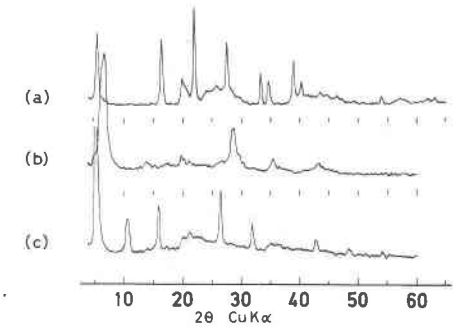

Fig. 3. X-ray diffraction patterns of surite. (a) Untreated, natural state; (b) the residue obtained from the sample powder pretreated with 0.75 percent hydrochloric acid, air-dried, filtrated; (c) the residue treated with ethylene glycol.

peak clearly expands to 17.6A after treatment with ethylene glycol (Fig. 3).

Heat effects

Heating below 550°C does not cause discernible changes in spacings and X-ray intensities (Fig. 4). At 550°C, all X-ray peaks are weakened without noticeable changes in spacings. At 650°C all peaks have disappeared and a broad rise at around 3.2A appears. Weak peaks from the heating product are discernible at 800°C. With the temperature rise in the region of 450°C or higher, the color of the sample turns to pale yellow, greenish-yellow, to green, probably due to the oxidation of lead ions. In the region of 650°C or higher, the sample tends to solidify, probably by partial fusion of a lead compound in the sample.

DTA and TG curves

DTA and TG curves simultaneously obtained are shown in Figure 5. As shown in Figure 5(a), the DTA curve of the sample in air has a sharp endothermic peak (A) at about 600°; two exothermic peaks, one (B) at about 700° and the other (C) at about 800°; and an endothermic peak (D) in the 700–800°C region. In the DTA curve of the sample in nitrogen, the two exothermic peaks (B) and (C) have disappeared and the endothermic peaks (A) and (D) remain behind, accompanying an inflection at about 800°C [Fig. 5(b)]. The (A) peak accompanies a clear weight loss. Gas analysis performed with nitrogen flowing at the temperature of (A) peak detected the evolution of CO_2 (not CO). The two exothermic peaks could not be assigned; they may be due to the oxidation of Pb ions at dehydroxylation stage of the 2:1 layer. The DTA and TG curves of surite are quite different from those of cerussite [Fig. 5(e)]. The peak temperature of the endothermic peak due to the evolution of CO_2, *i.e.* the disintegration of the carbonate structure, is about 300°C higher in surite than in cerussite. This may be due to the carbonate layer being bound in the interlayer region of the 2:1 layer. The DTA and TG curves of the residue agree with that of a smectite, showing a clear dehydroxylation peak at about 700°C [Fig. 5(c)]. For the sake of comparison, the DTA and TG curves of montmorillonite (a dioctahedral aluminum smectite) from Aterazawa, Yamagata Prefecture, are shown in Figure 5(d).

Infrared absorption spectra

The absorption bands (Fig. 6) at 1430, 840, and 690 cm^{-1} are assigned to carbonate, and a broad band at about 1000 cm^{-1} to silicate. Below 550°C, overall absorption bands do not suffer discernible changes in intensities and wave-numbers. At 650°C, they become weak and broad without discernible changes in wave-numbers. At 800°C, the bands at 840 and 690 cm^{-1} have disappeared but those of 1430 and 1000 cm^{-1} become broader but are still discernible, whereas X-ray peaks have entirely disappeared. At 1000°C the 1430 cm^{-1} band has disappeared, and the 1000 cm^{-1} band remains as a very broad peak. This suggests that the carbonate component decomposes prior to the silicate component.

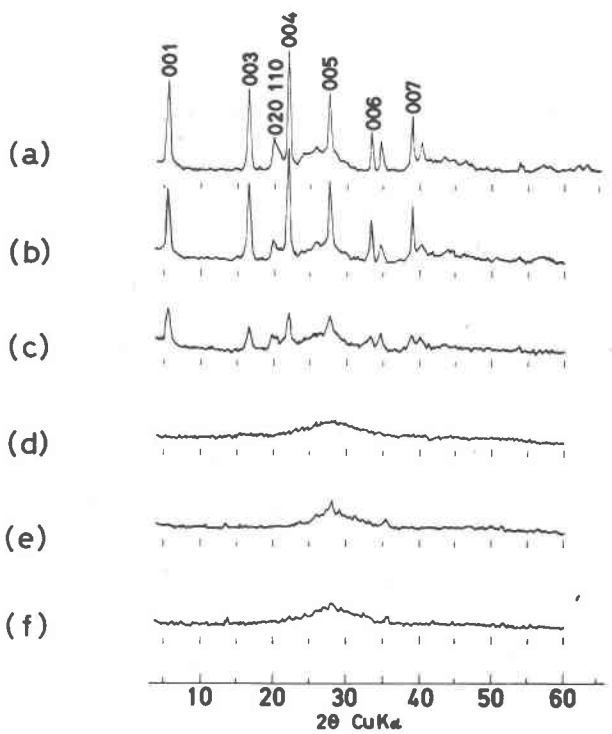

Fig. 4. Heat effects on X-ray powder diffraction patterns. (a) Room temperature; (b) 450°C; (c) 550°C; (d) 650°C; (e) 800°C; (f) 950°C.

Structural formula and structure model

The properties of surite strongly suggest that the mineral can be regarded as composed of the 2:1 layer of a dioctahedral smectite incorporated with a cerussite-like interlayer, because the mineral is found in association with cerussite. The cell dimensions of cerussite are $a = 8.468$, $b = 6.146$, $c = 5.166$A. The cell dimensions of a dioctahedral smectite such as montmorillonite, based on the orthogonal cell, may be given as follows:

$a = 5.18$–5.21, $\quad b = a\sqrt{3} = 8.97$–$9.02$,

$d(001) = 15$–17A

Thus the dimensions of the *ac* plane of cerussite are very close to those of the *ab* plane of montmorillonite minerals.

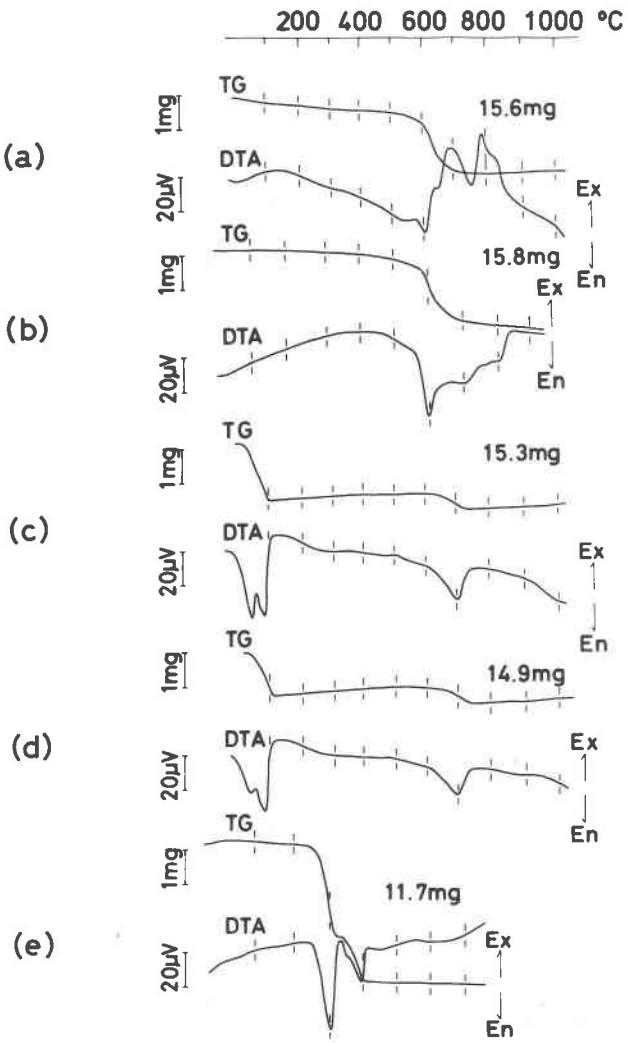

Fig. 5. DTA and TG curves: (a) surite, with air flowing; (b) surite, with nitrogen flowing; (c) the residue obtained from surite pre-treated with 0.75 percent hydrochloric acid, in air; (d) montmorillonite, in air; (e) cerussite, in air.

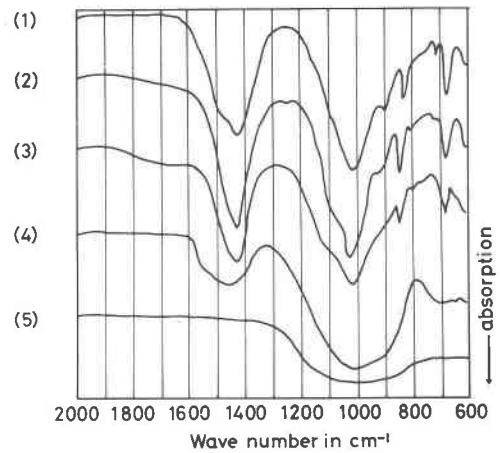

Fig. 6. Infrared absorption spectra of surite. (1) Untreated; (2) heated to 550°C; (3) heated to 650°C; (4) heated to 800°C; (5) heated to 1000°C.

Because of the 16.2A *c* dimension of surite, the most plausible model is one in which a cerussite layer with the thickness of its *b* dimension is intercalated between the 2:1 silicate layers of the montmorillonite lattice. To account for the other cell dimensions, the *ac* plane of the cerussite layer would be oriented parallel to the *ab* plane of the 2:1 layer of the montmorillonite structure; the *a* and *c* axes of the cerussite layer would be parallel to the *b* and *a* axes of the 2:1 layer of the montmorillonite structure respectively. A model in which CO_3 plane of the cerussite layer is in contact with the basal oxygen plane of the 2:1 layer is rejected because of the departure of calculated X-ray intensities from observed ones.

However, a structure model in which the Pb plane of the cerussite layer is in contact with the basal oxygen plane (Fig. 7) provides calculated X-ray intensities resembling observed ones.

The chemical composition of the residue obtained after treatment with 0.75 percent HCl can be transformed into the following formula of the smectite group:

$$W_{0.33}(Al_{1.70}Fe_{0.08}Mg_{0.36})(Si_{3.60}Al_{0.40})O_{10}(OH)_2 \quad (1)$$

and the most probable formula for surite is

$$(Pb_{1.90}Cu_{0.01}Ca_{0.25})(CO_3)_2(Al_{1.75}Fe^{3+}_{0.05}Mg_{0.30})(Si_{3.68}Al_{0.32})O_{10}(OH)_2 \quad (2)$$

The distribution of cations in the formula is adjusted as follows: (a) the anion number of CO_3 is 2.01 and the excess amount of 0.01 is excluded as an impurity,

Table 4. Observed and calculated structure factors of the 00*l* reflections of surite

00*l*	*d*(00*l*) (A)	*d*(001) (A)	$\|F\|_{obs}$*	F_{calc}**
1	16.2	16.2	94.0	-93.2
2				2.6
3	5.40	16.20	144.3	-58.3
4	4.05	16.20	210.3	213.6
5	3.240	16.20	199.6	-90.9
6	2.700	16.20	147.1	135.7
7	2.313	16.19	212.7	-151.1
8	2.024	16.22	85.9	-66.2
9	1.800	16.20	40.3	-41.2

Mean *d*(001)=16.20 A ; R=0.26

* *obtained from the relative intensities applied by the slit-correction (Table 2)*
** *obtained from the final z-parameters (Fig. 7)*

0.01 $CaCO_3$, and (b) the cation population on the lead carbonate interlayer is adjusted so as to give the total cationic charges of the lead carbonate layer close to 1/3.

On the basis of the model in Figure 7, X-ray intensities of the basal reflections were calculated in various cases where *z* parameters of ion planes and also ion contents in each plane were slightly modified in various possible extents. From the calculated data the writers could obtain the final *z* parameters shown in Figure 7, and the cell content expressed by a half cell as follows:

$$Pb_{1.75}(CO_3)_2(Al_{1.87}Fe_{0.05}Mg_{0.29})(Si,Al)_4O_{10}(OH)_2 \quad (3)$$

Table 4 shows the comparison of $F(00l)_{obs}$ with $F(00l)_{calc}$ and gives R = 0.26. Here, the cations on the Pb planes were represented by Pb ions only, without considering any isomorphous replacement. Pb planes are in two horizons: one is at the middle of the cerussite layer (inner Pb plane), and the other is in contact with the basal oxygen plane of montmorillonite (outer Pb plane). The distribution of Pb ions between the inner and outer Pb planes was obtained as $Pb^*_{0.85}Pb_{0.90}(CO_3)_2$, where Pb* is defined as Pb ions on the inner plane. An interlayer cationic charge of about 0.33 would be necessary. But such an interlayer charge is not obtained from the composition of $Pb_{1.75}(CO_3)_2$ without considering the uptake of Ca ions, a part of which would replace Pb ions and the remaining part would occupy some defect sites. It is difficult to determine the distribution of Ca ions between the inner and outer Pb planes. It may be reasonable to consider that the uptake of Ca ions is on the outer Pb plane, being nearer to the basal oxygen plane of montmorillonite than the inner Pb plane. To illustrate, the composition of $Pb^*_{0.85}Pb_{0.90}(CO_3)_2$ may be modified to $Pb^*_{0.85}(Pb_{0.78}Ca_{0.54})(CO_3)_2$, whereby an excess charge of about 0.33 is produced from the composition, and the number of electrons provided by the composition of $Pb_{0.78}Ca_{0.54}$ is equal to that provided by $Pb_{0.90}$. It is difficult to give final exact numerical values, but assuming that the inner Pb plane has no defect sites and contains only Pb ions, an ideal expression may be given as $Pb(Pb,Ca)_{1.17}(CO_3)_2$.

The results of the above considerations show that the chemical formula of surite may be given in the following ideal form;

$$Pb(Pb,Ca)_{1.17}(CO_3)_2(Al,Fe,Mg)_2(Si_{3.6}Al_{0.4})O_{10}(OH)_2 \quad (4)$$

The principles of this formulation are as follows: (a) the composition of the 2:1 layer is represented by that of the montmorillonite residue, or more strictly, a mineral on the montmorillonite–beidellite series; (b) it is also expected that a negative charge resulted from a net charge due to the 2:1 layer will be neutralized by an interlayer positive charge; (c) this interlayer charge will average 1/3, as shown in the minerals of the smectite group; (d) in surite, the interlayer charge will be created by the lead carbonate.

One-dimensional Fourier synthesis of electron density is shown in Figure 8. The *z* parameters (Fig. 7) show that the distance between the basal oxygen plane and the Pb plane is approximately 1.36A. This suggests that the Pb ions, radius 1.36A, are embedded in the hexagonal hole of the basal oxygens as is the case for potassium ions, radius 1.33A. The β-angle will be controlled by the displacement, $-a/3$, within the unit structure with the height of 16.2A. The angle is 96°4′ which is very close to the value 96.1°, obtained from electron diffraction patterns with aid of the X-ray powder-diffraction pattern.

We could not find a single crystal suitable for X-

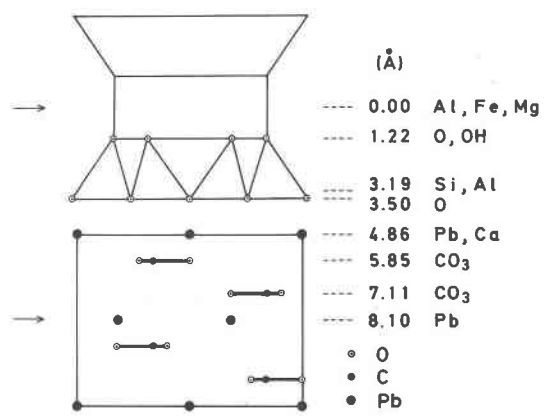

Fig. 7. Structural model of surite.

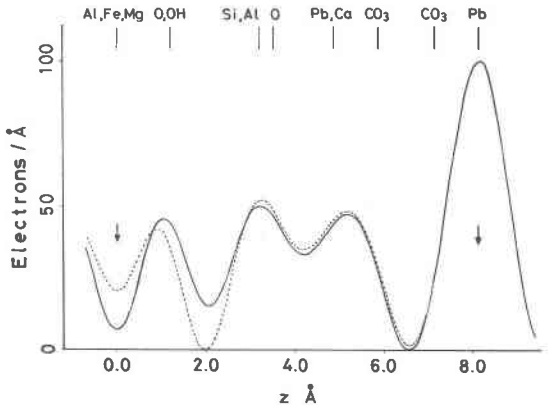

Fig. 8. One-dimensional Fourier synthesis of electron density normal to *ab* plane. Full line: observed; dotted line: calculated.

ray analysis. It is therefore difficult to make clear how the discrepancies of the lattice dimensions of cerussite and montmorillonite are harmonized on the stacking plane. A structure model in an ideal form can be made by considering that the *ab* dimensions of surite are applied to the structural dimensions of both cerussite and montmorillonite on the stacking plane. In such a model the Pb ions can be placed within the hexagonal holes of the basal oxygen plane. The symmetry of this structure model is governed only by the two-fold screw axes parallel to the *b* axis and then belongs to the space group $P2_1$. With respect to the structural dimensions and also to the chemical compositions, the interlayer material of surite may be termed "cerussite-like layer" rather than cerussite layer itself, as in the case of chlorite where the interlayer material is termed "brucite-like layer". The intensities of the (*hkl*) reflections calculated from this model are not inconsistent with the observed values.

Conclusion

The structure of surite is regarded as based upon a lead carbonate layer intercalated with the repetitive 2:1 silicate layers. The lead carbonate layer has essentially the structure of cerussite but the Pb sites are only partly occupied. The 2:1 silicate layer is essentially comparable with a dioctahedral smectite. The structure displays behavioral characters similar to both montmorillonite and chlorite but also different to both. The interlayer composition, the lack of solvation of the natural sample, and the lack of collapse on heating are definitely not like montmorillonite minerals. The stability of the interlayer and the lack of solvation or collapse are more like chlorite than montmorillonite. However, the tetrahedral composition expressed as Al(IV) = 0.3–0.4 is below the limit usually set for chlorite, and the interlayer composition is certainly not like chlorite. Therefore, since the interlayer is so different from any other layer silicate, surite should not be grouped with either montmorillonite or chlorite but should be in a category by itself.

Acknowledgments

Sincere thanks are offered to Professor S. W. Bailey, University of Wisconsin, for providing thoughtful comments and suggestions for this manuscript. The writers are also greatly indebted to Dr. Horacio Gatica of the Universidad Nacional del Sur, Argentina, and to Mr. Natalio Devicenzo of the Consejo Nacional de Investigaciones Cientificas y Tecnicas, Argentina. Thanks are extended to Assistant Professor Susumu Shimoda and Dr. Hiroshi Tateyama, Tokyo University of Education.

References

Hayase, K. and J. A. Dristas (1972) Presencia de mottramita en la zona de oxidacion del yacimiento de plomo, cobre y zinc, Mina Cruz del Sur, Los Menucos, Provincia de Rio Negro, Republica Argentina. *Rev. de la Asoc. Geol. Argentina, 27,* 300–308.

Manuscript received, December 1, 1977; accepted for publication, April 6, 1978.